J Struct Funct Genomics
DOI 10.1007/s10969-014-9191-0

X-ray structure of the mature ectodomain of phogrin

Martín E. Noguera · María E. Primo · Jean Jakoncic · Edgardo Poskus · Michele Solimena · Mario R. Ermácora

Received: 23 September 2014 / Accepted: 19 November 2014

Abstract Phogrin/IA-2β and ICA512/IA-2 are two paralogs receptor-type protein-tyrosine phosphatases (RPTP) that localize in secretory granules of various neuroendocrine cells. In pancreatic islet β-cells, they participate in the regulation of insulin secretion, ensuring proper granulogenesis, and β-cell proliferation. The role of their cytoplasmic tail has been partially unveiled, while that of their luminal region remains unclear. To advance the understanding of its structure–function relationship, the X-ray structure of the mature ectodomain of phogrin (ME phogrin) at pH 7.4 and 4.6 has been solved at 1.95- and 2.01-Å resolution, respectively. Similarly to the ME of ICA512, ME phogrin adopts a ferredoxin-like fold: a sheet of four antiparallel β-strands packed against two α-helices. Sequence conservation among vertebrates, plants and insects suggests that the structural similarity extends to all the receptor family. Crystallized ME phogrin is monomeric, in agreement with solution studies but in striking contrast with the behavior of homodimeric ME ICA512. The structural details that may cause the quaternary structure differences are analyzed. The results provide a basis for building models of the overall orientation and oligomerization state of the receptor in biological membranes.

Keywords Insulin · Secretory granule · Dense-core vesicle · Peptide hormone · Diabetes

Abbreviations

ME	Mature ectodomain
ICA512	Islet cell autoantigen 512

Introduction

Protein-tyrosine phosphatases (PTP) have pivotal roles in signal transduction and therefore in the regulation of many processes, such as cell division, growth, differentiation, and metabolism. These enzymes can be either soluble

Electronic supplementary material The online version of this article (doi:10.1007/s10969-014-9191-0) contains supplementary material, which is available to authorized users.

M. E. Noguera · M. R. Ermácora (✉)
Departamento de Ciencia y Tecnología, Universidad Nacional de Quilmes, Sáenz Peña 352, B1876BXD Bernal, Buenos Aires, Argentina
e-mail: ermacora@unq.edu.ar

M. E. Primo · E. Poskus
División Endocrinología del Hospital de Clínicas J. de San Martín, Facultad de Farmacia y Bioquímica, Instituto de Estudios de la Inmunidad Humoral, Universidad de Buenos Aires–Conicet, Bernal, Argentina

J. Jakoncic
Brookhaven National Laboratory, Upton, NY, USA

M. Solimena
Paul Langerhans Institute Dresden, Uniklinikum Carl Gustav Carus, Dresden University of Technology, Dresden, Germany

M. Solimena
Max Planck Institute of Molecular Cell Biology and Genetics, 01307 Dresden, Germany

M. R. Ermácora
Instituto Multidisciplinario de Biología Celular, Conicet, Calle 526 y Camino General Belgrano, B1906APO La Plata, Buenos Aires, Argentina

Published online: 26 November 2014

(cytoplasmic) or transmembrane, i.e. receptor-like (RPTP). The latter comprise type-1, transmembrane proteins that participate in cell–cell and cell–matrix contacts, and possess a diversity of adhesive and multimerization modules. Some of them have been found to be involved in human diseases such as cancer, autoimmunity, and degenerative disorders [1–3].

Phogrin (also known as IA-2β, IAR, ICAAR, or PTPRN2) and ICA512 (also known as IA-2, PTP35, or PTPRN) are closely related RPTP located in dense core vesicles of brain, pituitary, pancreatic islets, and adrenal endocrine cells. Both are inactive tyrosine phosphatases, as a consequence of highly conserved active site mutations. Recently, however, it was reported that phogrin dephosphorylates phosphatidylinositol [4].

In the β-cell, phogrin and ICA512 are involved in the biogenesis, cargo storage, traffic, exocytosis and recycling of secretory granules, as well as in β-cell proliferation [5–11]. Also they are major autoantigens in type-I diabetes mellitus, and the corresponding autoantibodies are widely used markers for early detection of individual at risk of the disease [12–14].

In mice, gene deletion of ICA512, phogrin, or both, causes alterations in glucose tolerance tests, decreased glucose-stimulated insulin secretion, abnormal secretion of pituitary hormones and female infertility [15–17]. Importantly, the insulin content of β-cells in double knockout mice is about fifty percent less than in controls [18].

Despite being closely related, phogrin and ICA512 have different expression profiles: ICA512 expression increases during development and is influenced by glucose, insulin, cAMP-generating agents and proinflammatory cytokines; in contrast, phogrin expression is not significantly affected by glucose levels [19–23].

The precursors of ICA512 and phogrin are polypeptides of about 1,000 residues that after proteolytic processing by furin-like convertases along the secretory pathway result into ~60-kDa transmembrane mature proteins [5]. The mature transmembrane fragment (TMF) includes an N-terminal ectodomain (ME) oriented toward the lumen of the granule, a transmembrane domain (TM), and a cytoplasmic tail of about 45 kDa. The cytoplasmic tail comprises a juxtamembrane segment and the PTP domain distinctive of the RPTP family (Fig. 1). mature ectodomain (ME phogrin) and ME ICA512 face the extracellular space during insulin secretion and therefore are obvious candidates for ligand-receptor interactions and for oligomerization.

Homo- and hetero-dimerization are common among type-I membrane receptors, and particularly for the RPTP family of proteins. Among the latter, phogrin and ICA512 form homo- and heterodimers and can associate with other RPTP members. This oligomerization has been postulated

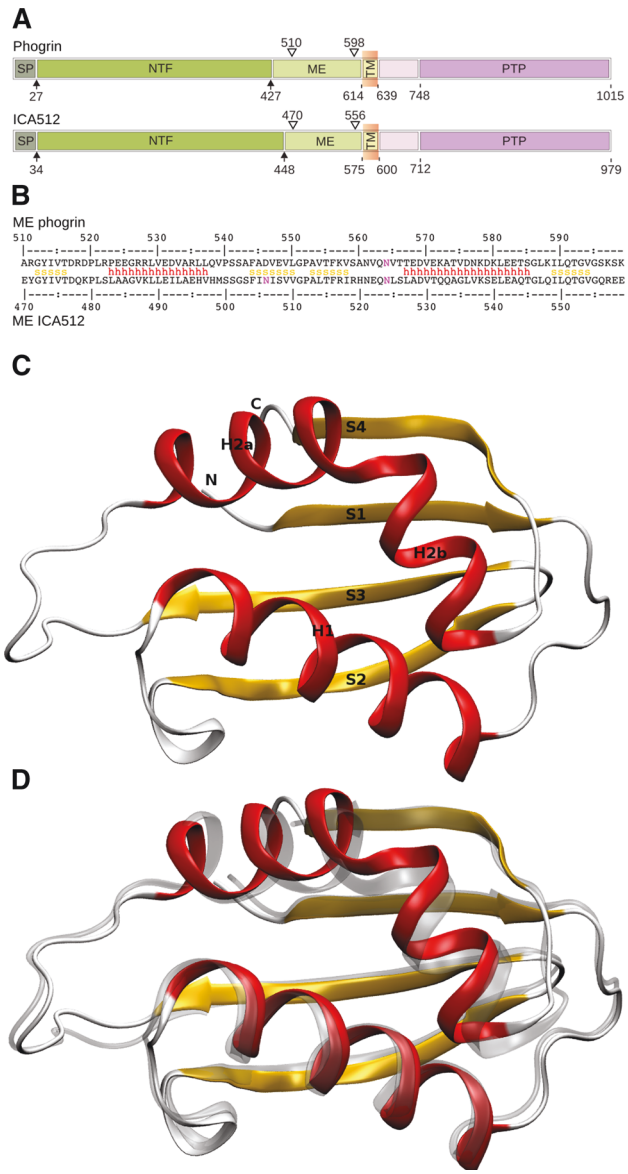

Fig. 1 **a** Outline of the domain organization of phogrin and ICA512. *Solid arrow heads* show signal peptidase and prohormone convertases processing sites that remove the signal peptide (SP) and the N-terminal fragment (NTF) and result in the production of the mature transmembrane fragment. The latter comprises the mature ectodomain (ME), the transmembrane region (TM), and the cytoplasmic segment with the phosphatase (inactive) domain (PTP). The boundaries of these receptor regions are indicated by residue numbers. In addition, *open arrow heads* show the limits of the X-ray structure fragments described in this work. **b** Aligned sequences corresponding to the segments indicated by *open arrows in Panel A*. Secondary structure determined in this work for ME phogrin (α-helix, *h, red*; β-strand, *s, gold*) is shown. Pedicted sites of *N*-glycosylation are in *purple*. **c**. *Ribbon* representation of the structure of ME phogrin. The single chain in the asymmetric unit of the crystal at pH 7.4 is shown (PDB ID: 4HTI); however, the backbone structure at pH 4.6 is nearly identical (PDB ID. 4HTJ). *Coloring* is according to secondary structure with β-strands in *gold*, helices in *red* and aperiodic structure in *white*. The order of the strands and helices is indicated S1–S4 and H1–H2, respectively. **d** Backbone superposition of ME phogrin and ME ICA512. ME phogrin is the same as in *Panel C*, and ME ICA512 (in *transparent silver*) corresponds to PDB ID: 3N01 [27]

as a general regulatory mechanism for RPTP, and supporting this notion it was found that co-expression of phogrin or ICA512 with RPTPα reduces the phosphatase activity of the latter [24]. The cytoplasmic tails of phogrin and ICA512 are capable of homo- and hetero-dimerization with the contribution of both the juxtamembrane and the PTP segments. The association is also detected when assayed with the whole receptors, and moreover, the TM domains have a significant potential for self-interaction in the membrane [24, 25].

Recently, we determined the X-ray structure of 89 of the 127 residues of ME ICA512 [26, 27]. This domain, turned out to be related to the SEA (Sea-urchin sperm protein, Enterokinase, Agrin) module, which is specialized for oligomerization and interaction with the extracellular matrix [28]. This finding simplified the classification of the RPTP family because, with the single exception of the subtype R7 (PCPTP1), all RPTP are now characterized by having extracellular modules for the interaction with the extracellular matrix and cell-to-cell contact.

Crystallography provided the basic structural information and a model for the homo-dimerization modes that may be of functional importance for ME ICA512. In addition, previous work provided the basic biochemical and biophysical information on both ME phogrin and ME ICA512 [29, 30]. Moreover, although the sequence similarity of ME phogrin is 63 %–high enough as to safely assume a common overall fold– some of the differences in expression, regulation, and function between ICA512 and phogrin might be related to specific sequence changes or subtle structural details. To unify and systematize the structural and biophysical information regarding these proteins, we undertook the resolution of the X-ray structure of human ME phogrin. The results may help in the long-term efforts to unveil the architecture of the whole receptor inserted in biological membranes.

Experimental procedures

Molecular visualization and calculations were performed with VMD [31]. Pockets and cavities properties were calculated using CASTp [32]. Electrostatic potentials were calculated using APBS and PDB2PQR [33]. Residue pKa were calculated with PROPKA3.0 [34].

Protein expression and purification

Cloning, expression in *E. coli,* and purification of ME phogrin (residues 502–599 of human phogrin, UniProt ID: Q92932) have been described [30]. Buffer exchange to 10 mM Tris–HCl, pH 7.4 and protein concentration were accomplished with an Amicon 4 device (Millipore, Bedford, MA, USA) with a 10 kDa cut-off.

Crystallization

Crystals of ME phogrin were obtained at 20 °C using the hanging-drop method in two different conditions. The drop (2 µl) was a 1:1 blend of protein and reservoir solution (1 ml). The reservoir solution for the first condition was 0.2 M ammonium sulphate, 30 % PEG 4000, and for the second condition it was 0.1 M sodium acetate pH 4.6, 0.2 M ammonium sulphate, 25 % PEG 4000. Crystals appeared after one and 3 days for the first and second condition, respectively. Prior to data collection, first-condition crystals were flash-cooled without cryo-protectant in liquid nitrogen. Crystals from the second condition were cryo-protected by soaking in the mother liquor supplemented with 25 % glycerol before flash-cooling.

Data collection and processing

The X-ray diffraction data were collected at 100 K on the X6A beam line at the National Synchrotron Light Source (NSLS), using an ADSC Q270 detector (Area Detector Systems Corp., Poway, CA, USA). Indexing, integration, scaling and reduction were performed using the HKL2000 suite of programs [35]. Five percent of the measured reflections were flagged for cross-validation. Data collection and processing statistics are summarized in Table 1.

Structure solution, refinement and validation

The structures were solved by molecular replacement using the coordinates of ME ICA512 (PDB ID: 2QT7; RCSB PDB, www.rcsb.org; [26]) as the starting model. The solution was obtained using MOLREP [36] as implemented in the MrBump program [37] from the CCP4 suite [38]. Refinement was carried out using REFMAC5 [39] interspersed with manual model building using Coot [40]. B-factors of protein atoms were treated using TLS refinement. With the first crystal, one group per chain was sufficient to account for the anisotropy of atomic displacement parameters; whereas for the second crystal (at pH 4.6), 14 groups of TLS were used, using the TLSMD server to help the partition into multiple segments [41]. The stereochemical quality of the model was verified using the Molprobity server [42]. The atomic coordinates and structure factors have been deposited in the Protein Data Bank (PDB ID: 4HTI, 4HTJ).

Table 1 Data collection, phasing and refinement statistics

Sample information		
pH	7.4	4.6
PDB entry	4HTI	4HTJ
Data collection[a]		
Synchrotron	NSLS	NSLS
Wavelength (Å)	0.91840	0.91840
Space group	$P6_122$	$P6_122$
Unit cell dimensions (Å)	$a = b$=55.133; $c = 148.39$	$a = b = 54.742$; $c = 149.147$
Unit cell angles (°)	$\alpha = \beta$=90.00; $\gamma = 120.00$	$\alpha = \beta$=90.00; $\gamma = 120.00$
Resolution limits (Å)	30.00–1.95 (1.98–1.95)	20.00–2.01 (2.03–2.00)
R^{b}_{merge}	0.06 (0.99)	0.06 (0.79)
Mean I/σ (*I*)	104.6 (7.72)	41.2 (3.6)
Completness (%)	99.6 (100)	95.4 (61.9)
Redundancy	40.5 (41.4)	12.5 (9.7)
Matthew's coefficient (Å^3/Da)	3.01	2.98
% solvent	59.17	58.79
Molecules per ASU	1	1
Refinement		
Resolution limits (Å)	30.00–1.95	20.00–2.01
Number of reflections	10,292	9,206
$R_{work}/R^{c,d}_{free}$	0.221/0.243	0.203/0.238
Protein atoms	670	676
Water molecules	40	34
Protein atoms average *B–factors* (Å^2)	48.5	46.7
Water molecules average *B–factors* (Å^2)	45.6	48.7
Bond length *RMSD* (Å)	0.021	0.019
Bond angles *RMSD* (°)	1.563	2.000
Ramachandran plot		
Most favoured φψ pairs (%)	100	100

[a] Data were collected on a single crystal. Values in parentheses are for the highest-resolution shell

[b] $R_{merge} = \sum_{hkl} \sum_i |I_{hkl,i} - \langle I_{hkl} \rangle| / \sum_{hkl} \sum_i I_{hkl,i}$

[c] $R_{work} = \sum |F_{obs} - F_{calc}| \sum |F_{obs}|$, where F_{calc} and F_{obs} are the calculated and observed structure factor amplitudes, respectively

[d] R_{free} is the same as R_{work}, but calculated for 5.0 % of the total reflections (chosen at random and omitted during refinement)

Results and discussion

Structure determination and fold features

The structure of ME phogrin at pH 7.4 and 4.6 was solved at 1.95- and 2.01-Å resolution, respectively. ME phogrin crystals belong to the hexagonal space group $P6_122$, and the asymmetric unit contains a single peptide chain (residues 510–598) with overall dimensions 22 × 25 × 35 Å^3 (Fig. 1). Residues 501–509 and 599, at the N- and C-termini showed no electron density and are presumably disordered. The backbone structure is nearly identical at both pH (all backbone atom RMSD = 0.29 Å). As well, the backbone structure of ME phogrin is nearly identical to that we reported previously for ME ICA512 [26, 27] (RMSD of 0.80–1.16 Å; Fig. 1). In the cell, ME phogrin and ICA512 are first within the endoplasmic reticulum and the Golgi cisternae, subsequently in the SG lumen where they are exposed to changes in the local H^+ concentration up to pH ~4.5, and finally they face the extracellular space and return to a neutral pH. The high degree of similarity between the phogrin structures at pH 7.4 and 4.6 suggests that, as found with ME ICA512, there are no significant pH dependent conformational changes associated with the maturation of the granule and posterior insulin secretion.

The fold of ME phogrin and ME ICA512 is classified in SCOP2 [43] as ferredoxin-like (βαββαβ; 2 layers, α/β; antiparallel β–sheet, order: 4132; CF:2000014). The ferredoxin-like fold–a layer of four antiparallel β-strands onto which a second layer of two α-helices is packed– is ubiquitous and shared by many protein domains of very different origins and functions. These domains, grouped into several superfamilies, differ in the details of secondary structure elements mutual orientation, length, and in the elaborateness of the connecting loops.

Interestingly, ME phogrin and ME ICA512 fold is most similar to that of the SEA superfamily. For instance, the MUC1 SEA domain from the human transmembrane protein mucin [44] can be superposed to ME phogrin with a RMSD of 1.75 Å (PDB ID: 2ACM; 56 % of the backbone atoms, not shown). This strong structural similitude is likely to be relevant biologically, because mucin's SEA domains have several additional features in common with ME phogrin and ME ICA512: they are proximal to the plasma membrane facing the extracellular matrix and undergo complex posttranslational processing and proteolysis.

Sequence and structure similarity within the receptor family

Based on sequence similarity, ME phogrin and ME ICA512 have been classified in Pfam [45] as part of the Receptor_IA-2 (PF11548) family, which includes mammals, amphibian, fish, insect, and plant members. We have previously shown that the Receptor_IA-2 and SEA (PF01390) families are related and can be recognized by a single HMM profile [16]. In this regard, ME phogrin and ME ICA512 share 42 % amino acid identity, whereas distant members share with human ME phogrin about 26 %

sequence identity (see Fig. 1 in online resources). The X-ray results made possible to examine the structural and functional significance of sequence conservation. In Fig. 2 it is shown the spatial disposition of invariant and highly conserved amino acid positions. This information is examined below, in concert with the structural details.

Packing and electrostatic details

The β-sheet and the two α-helices of ME phogrin (Fig. 1) enclose an extended hydrophobic core made by well-packed, highly-conserved aliphatic and phenyl side chains. About 30 % of the residues are involved in the formation of this hydrophobic core. This suggests high stability and low conformational flexibility of the domain as a whole, which is consistent with its resistance to proteolysis [30] and a role as a robust structural scaffold for putative protein–protein interactions.

Surface electrostatic potentials of ME phogrin and ME ICA512 are shown in Fig. 3. ME phogrin is acidic, with a calculated pI for both the folded and unfolded structure of 4.86. Similar results were obtained for ME ICA512, with a pI 5.56 and 5.68 for the folded and unfolded states, respectively. Interestingly, both proteins exhibit two equivalent charged surfaces at opposite sides. The predominantly positive surface corresponds to the exposed side of the β-sheet (right panels in Fig. 3); the opposite, predominantly negative surface corresponds to the polar side of the two helices (left panels in Fig. 3).

In nearly all the receptor family members, the N- and C-terminal segments that precede and follow the solved structure are rich in acidic residues (not shown). In the whole receptor inserted in the membrane, these segments may be juxtaposed to the positive face mentioned above and thus stabilizing the whole structure. The significance of the negative face is less clear, however it may be part of a binding site for metals or other positively charged ligands in the lumen of the secretory granule. In the phogrin crystallization milieu no metals were present and no electronic density compatible with bound metals was observed. Nevertheless, the negative face exhibits a potential metal binding site observed before occupied with calcium in several crystals of ME ICA512. This binding site formed by Asn-564 *O* and Asp-569 *OD* atoms –in a loop that will be described with more detail below–seems to be conserved in most of the receptor family members at the N-terminus of α-helix 2.

The inspection of the electrostatic potentials led to the identification of specific charged side chains that are almost invariant in all the receptor family (Figs. 3, and Fig. 1 in online resources): Lys 578 and Glu 582 on the predominantly negative surface and Lys 557 on the positive one. The persistence among the species of these specific charges at the protein surface suggests their possible involvement in biological function or recognition.

The structural role of core residues justifies their preservation across the species; on the other hand, preserved non-core residues may provide clues for biological function. In this regard, β-strand 2 and 3 (Fig. 1) and the intervening *type II L* β-turn contain several invariant or highly-preserved residues. Indeed, this tight turn is one of the distinctive structural hallmarks of this receptor family relative to other SEA domains. In MUC1 a two-residue insertion in this turn introduces a conformational stress that results in protein self-proteolysis [44]. Insertions at this turn are also seen in MUC16 [46] and in dystroglycan [47],

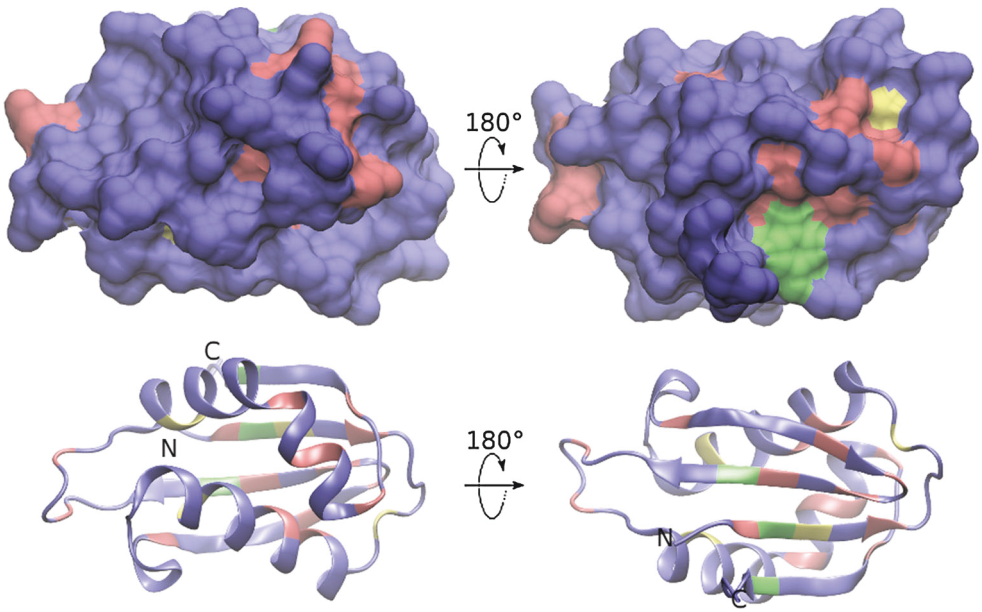

Fig. 2 Invariant and highly conserved residues in ME phogrin and ME ICA512. The assignment is based in a sequence alignment of 65 representative members (Pfam Receptor_IA-2 family PF11548); Fig. 1 in on line resources). The three invariant residues (Y513, F556, G593; phogrin numeration) are shown in *green*. Sixteen and two residues invariant in 95 and 90 % of the cases are shown in *coral* and *yellow*, respectively. *Left and right panels* are surface and *ribbon* representations of phogrin structures related by a 2-fold rotation along an horizontal axis

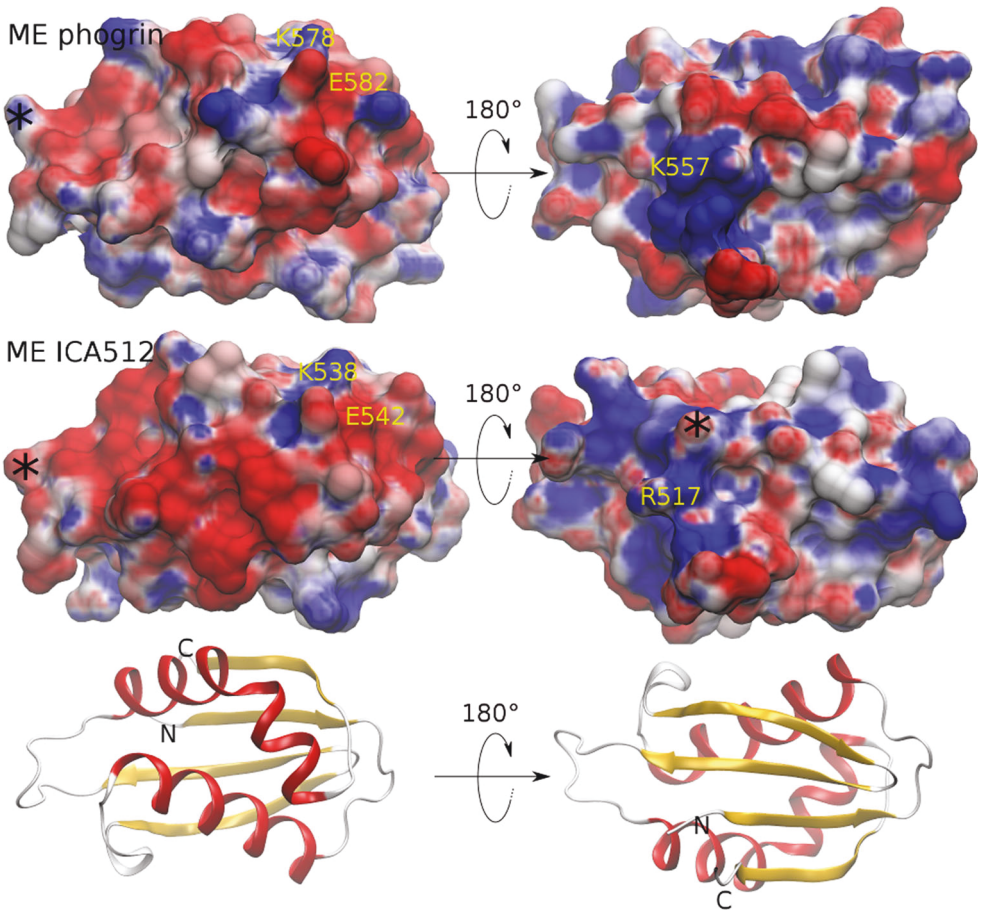

Fig. 3 Surface electrostatic potentials of ME phogrin and ME ICA512. Two opposite faces are shown colored according to the electrostatic potential (from *blue* +5 kT/e to *red* −5kT/e). On the *bottom*, a *ribbon* representation of the above molecular orientations is given. *Asterisks* indicate known N-glycosilation sites (two in ME ICA512 and one in ME phogrin). The *asterisks* on the *left panel* also mark the region of the NG loop, described in the text as a potentially relevant site for binding and interaction. Specific charged residues that are almost invariant in the receptor family are labeled in *yellow*

in both cases with an impact in the local geometry of the β-sheet.

The *N*-glycosylation site

Another hallmark of the receptor family is the protruding eight-residue segment that connects β-strand 3 and α-helix 2 (Fig. 4), and which we denominate 'NG loop'. The NG loop includes preserved Asn, Ser, Thr, and Gln residues (one of them is a *N*-glycosylation site), and the putative metal binding site mentioned previously. It is also a highly-structured loop conforming to the structural *Asx motif* [48] with an extensive net of hydrogen bonds between Asn side chains and backbone *NH* and *O* atoms. However, the most striking property of the NG loop is that it exposes a shallow negative cavity rimmed by four backbone *O* atoms as intramolecularly-unsatisfied hydrogen-bond acceptors (see the left panel of Fig. 3). Contributing to this electrostatically negative rim are also the C-cap of helix 1–with several unsatisfied main chain hydrogen-bond acceptors–and its macrodipole. All together, these conserved exceptional

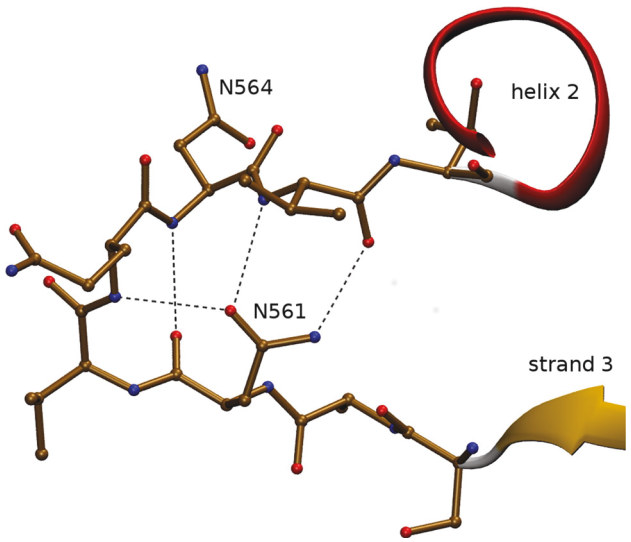

Fig. 4 The structure of the NG loop. The segment connecting β-strand 3 and α-helix 2 is sequentially well preserved among the receptor family and exhibits interesting electrostatic and hydrogen-bonding properties (see the text). This protein region is proposed as the binding site for a still unidentified ligand

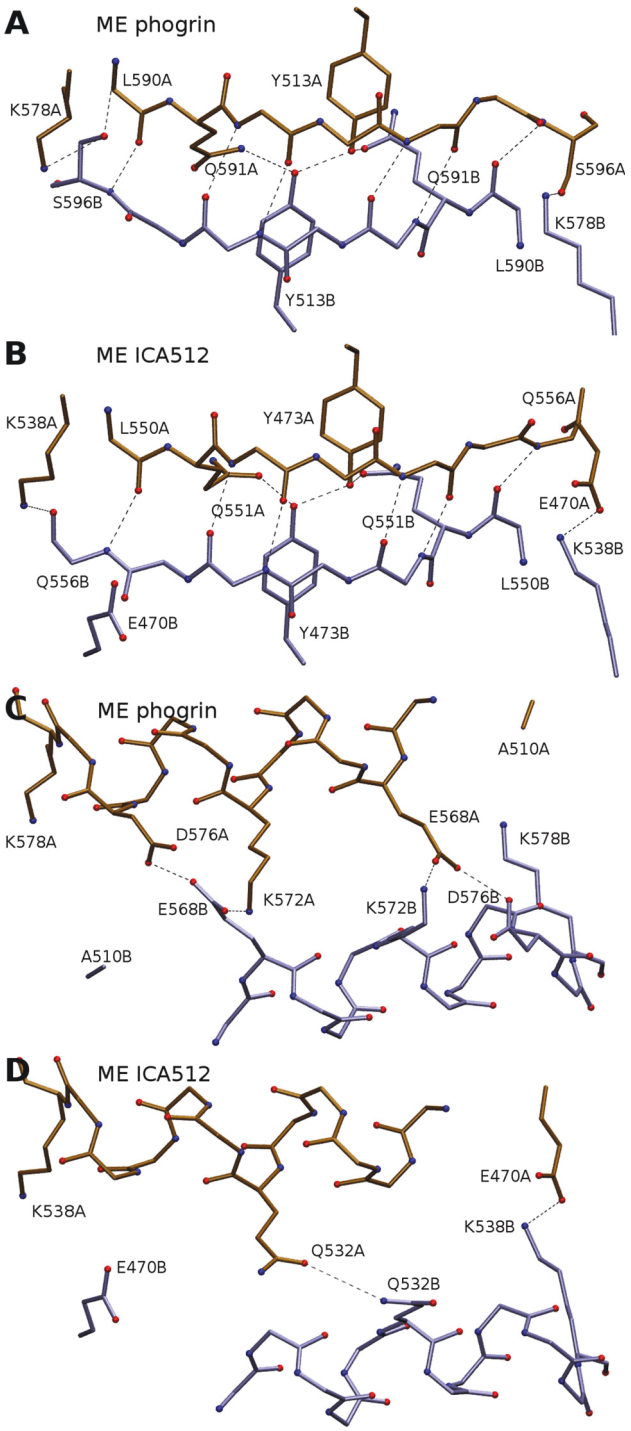

◀**Fig. 5** β4–β4 dimerization interface. The hydrogen-bond network stabilizing the interaction between strands β4 in the crystal structure of ME ICA512 is shown in (**b**). In (**a**) a modeled (hypothetical) β4–β4 interaction for phogrin is presented. The ME phogrin model was prepared simply by placing two of the experimentally determined phogrin monomers as if they were to form the β4–β4 dimer observed for ME ICA512. In (**c**, **d**), additional interactions in the β4–β4 dimerization interface involving helix 2 are depicted. As in the first two panels, *Panel D* shows the experimentally determined hydrogen bond pattern in ME ICA512, whereas in *Panel C* the modeled equivalent interaction for phogrin is proposed. Only very minor rotameric adjustments were needed to achieve robust geometric consistency of the models. Note that some side chains has been omitted for clarity and that all the panels represent partial aspects of the same orientation of the dimers. Almost most residues in the interface are identical in the two proteins, and that the few mutations results in the conservation of the hydrogen-bond pattern

structural features suggest a surface spot that is likely to be an important binding site for yet unidentified ligands.

Putative dimerization interfaces

As mentioned in the *Introduction*, to understand the architecture of the whole RPTP inserted in the membrane is crucial to characterize the dimerization mode of ME phogrin and ICA512 and the differences thereof. Most of the experimental evidence gathered so far is related to ICA512 and can be summarized as follows.

Unglycosylated ME ICA512 forms a dimer in solution through a β-sheet extension mediated by the hydrogen-bond antiparallel pairing of β-strand 2 from different monomers; we termed this dimer 'β2–β2′ [26, 27]. A second dimerization mode of ME ICA512 is mediated by a similar pairing of β-strand 4 to form the 'β4–β4′ dimer; however this second association mode depends of additional stabilizing forces, as those present in the crystalline state, or those potentially driven by the dimerization of the other receptor domains [26, 27]. Nevertheless, the predicted glycosylation at Asn 506 should sterically hinder the formation of a ME ICA512 β2-β2 dimer, and therefore the existence of such dimer in the mature form of the receptor should be considered unlikely.

In a recent work, using size-exclusion chromatography and multi-angle ligth-scattering we demonstrated that ME phogrin is a monomer in solution [16]. Since the existence of a monomeric state of the whole receptor inserted in the membrane is counterintuitive and in disagreement with evidences of self-association of the transmembrane and cytoplasmic domains, it seems proper to assume that, in the cell, ME domains will also interacts homodimerically in both the mature forms of phogrin and ICA512. That is why the experimental findings that ME phogrin is a monomer also in the crystals was at first surprising.

The lack of β2–β2 dimer formation in phogrin is, however, readily explained by crucial sequence differences at the interface. β2-strand in ME ICA512 establishes two symmetric interchain hydrogen bonds through the side chains of Asn 506 and Ser 508. These residues correspond to Asp 546 and Glu 548 in phogrin, which results not only in the loss of two stabilizing hydrogen bonds but in the concentration of four voluminous and negatively charged side chains in a small and closely packed region of the interface (not shown). Furthermore, the β2–β2 interface comprises the antiparallel

pairing of helix 1, which extends the hydrophobic core across the two monomers. In this association core, Arg 527 of phogrin replaces Val 487 in ICA512, resulting in the burial of two closely packed and unbalanced positive charges (not shown). These changes are likely to cause a very large destabilization of a β2–β2 interface in phogrin. It is important to note that the sequence changes that make the β2–β2 phogrin interface inviable are characteristic of all ME from the RPTPN2 gene.

Unlike the β2–β2 interface, β4–β4 dimerization involves strand residues that are almost perfectly conserved in ICA512 and phogrin (Fig. 1 in online resources). A model (Fig. 5, panels A and B) shows that a β4–β4 interaction in ME phogrin would be equivalent to that experimentally observed in ME ICA512.

β4–β4 dimerization also involves the antiparallel pairing of α-helix 2 (*H2a* in Fig. 1) and the prolongation of the hydrophobic core across the dimerization interface (not shown). Despite that in the interacting helical segment there are several sequence differences between phogrin and ICA512, these remain favorable with dimerization. Indeed, if an effect should be expected, this would be a strengthening of the interaction. For instance, the single cross-over hydrogen bond Gln 532A—Gln 532B in the dimer of ME ICA512 becomes a multiple bridge Glu 568A—Asp 576B, Glu 568A—Lys 572B, and Glu 568B—Asp 576A, Glu 568B—Lys 572A (Fig. 5, panels C and D).

The mentioned structural details predict a viable β4–β4 dimerization in ME phogrin. However, its realization, as in the crystal of ME ICA512, may depend on additional stabilization forces arisen from cooperative interactions between the transmembrane and cytoplasmic domains in the membrane-inserted receptor.

Concluding remarks

All the above results allow us to draw the following conclusions. The structure of ME phogrin and ME ICA512 are remarkably similar, despite the sequence differences between them. The sequence conservation between the ME domains of representative members suggests that the structural similarity extends to all the family. The quaternary structure of ME domains, however, may be different. Notably, the β2–β2 dimerization mode present in solution and in the crystalline state of ICA512 is not realized in phogrin. On the contrary, β4–β4 dimerization seems feasible from a structural point of view in both kind of receptors; the fact that so far its existence has been demonstrated only in the crystalline state of ICA512 may indicate that further interactions should take place for its realization in phogrin. Finally, the structural characterization of ME phogrin presented herein, along with the previous studies on ICA512, provides a basis for building models of the overall orientation and oligomerization state of the receptor in biological membranes. These models in turn should help in the design of experiments aimed to test the functioning of the receptor in the cell.

Acknowledgments This work was supported by the Consejo Nacional de Investigaciones Científicas y Técnicas, (grant number 11220090100044), the Universidad Nacional de Quilmes (grant number 0675/09), the DFG Research Exchange Program Germany-Argentina N. 444ARG113/9/1-0, and the BMBF Network of Competence for Diabetes Research. X-ray data collection at beamline X6A of the National Synchrotron Light Source was supported by NIH grant GM-0080 and DOE contract DE-AC02–98CH10886.

References

1. Andersen JN, Mortensen OH, Peters GH, Drake PG, Iversen LF, Olsen OH, Jansen PG, Andersen HS, Tonks NK, Moller NP (2001) Structural and evolutionary relationships among protein tyrosine phosphatase domains. Mol Cell Biol 21:7117–7136
2. Andersen JN, Jansen PG, Echwald SM, Mortensen OH, Fukada T, Del Vecchio R, Tonks NK, Moller NP (2004) A genomic perspective on protein tyrosine phosphatases: gene structure, pseudogenes, and genetic disease linkage. FASEB J 18:8–30
3. Brady-Kalnay SM, Tonks NK (1995) Protein tyrosine phosphatases as adhesion receptors. Curr Opin Cell Biol 7:650–657
4. Caromile LA, Oganesian A, Coats SA, Seifert RA, Bowen-Pope DF (2010) The neurosecretory vesicle protein phogrin functions as a phosphatidylinositol phosphatase to regulate insulin secretion. J Biol Chem 285:10487–10496
5. Trajkovski M, Mziaut H, Altkrüger A, Ouwendijk J, Knoch K, Müller S, Solimena M (2004) Nuclear translocation of an ICA512 cytosolic fragment couples granule exocytosis and insulin expression in β-cells. J Cell Biol 167:1063–1074
6. Trajkovski M, Mziaut H, Schubert S, Kalaidzidis Y, Altkrüger A, Solimena M (2008) Regulation of insulin granule turnover in pancreatic beta-cells by cleaved ICA512. J Biol Chem 283:33719–33729
7. Mziaut H, Kersting S, Knoch K, Fan W, Trajkovski M, Erdmann K, Bergert H, Ehehalt F, Saeger H, Solimena M (2008) ICA512 signaling enhances pancreatic beta-cell proliferation by regulating cyclins D through STATs. Proc Natl Acad Sci USA 105:674–679
8. Torii S, Saito N, Kawano A, Hou N, Ueki K, Kulkarni RN, Takeuchi T (2009) Gene silencing of phogrin unveils its essential role in glucose-responsive pancreatic beta-cell growth. Diabetes 58:682–692
9. Torii S (2009) Expression and function of IA-2 family proteins, unique neuroendocrine-specific protein-tyrosine phosphatases. Endocr J 56:639–648
10. Schubert S, Knoch K, Ouwendijk J, Mohammed S, Bodrov Y, Jäger M, Altkrüger A, Wegbrod C, Adams ME, Kim Y, Froehner SC, Jensen ON, Kalaidzidis Y, Solimena M (2010) β2-Syntrophin is a Cdk5 substrate that restrains the motility of insulin secretory granules. PLoS ONE 5:e12929
11. Suckale J, Solimena M (2010) The insulin secretory granule as a signaling hub. Trends Endocrinol Metab 21:599–609
12. Lu J, Li Q, Xie H, Chen ZJ, Borovitskaya AE, Maclaren NK, Notkins AL, Lan MS (1996) Identification of a second transmembrane protein tyrosine phosphatase, IA-2beta, as an autoantigen in insulin-dependent diabetes mellitus: precursor of the 37-kDa tryptic fragment. Proc Natl Acad Sci USA 93:2307–2311

13. Solimena M, Dirkx RJ, Hermel JM, Pleasic-Williams S, Shapiro JA, Caron L, Rabin DU (1996) ICA 512, an autoantigen of type I diabetes, is an intrinsic membrane protein of neurosecretory granules. EMBO J 15:2102–2114
14. Bottazzo GF, Bosi E, Cull CA, Bonifacio E, Locatelli M, Zimmet P, Mackay IR, Holman RR (2005) IA-2 antibody prevalence and risk assessment of early insulin requirement in subjects presenting with type 2 diabetes (UKPDS 71). Diabetologia 48:703–708
15. Saeki K, Zhu M, Kubosaki A, Xie J, Lan MS, Notkins AL (2002) Targeted disruption of the protein tyrosine phosphatase-like molecule IA-2 results in alterations in glucose tolerance tests and insulin secretion. Diabetes 51:1842–1850
16. Kubosaki A, Gross S, Miura J, Saeki K, Zhu M, Nakamura S, Hendriks W, Notkins AL (2004) Targeted disruption of the IA-2beta gene causes glucose intolerance and impairs insulin secretion but does not prevent the development of diabetes in NOD mice. Diabetes 53:1684–1691
17. Kubosaki A, Nakamura S, Notkins AL (2005) Dense core vesicle proteins IA-2 and IA-2beta: metabolic alterations in double knockout mice. Diabetes 54(Suppl 2):S46–S51
18. Henquin J, Nenquin M, Szollosi A, Kubosaki A, Notkins AL (2008) Insulin secretion in islets from mice with a double knockout for the dense core vesicle proteins islet antigen-2 (IA-2) and IA-2beta. J Endocrinol 196:573–581
19. Seissler J, Nguyen TB, Aust G, Steinbrenner H, Scherbaum WA (2000) Regulation of the diabetes-associated autoantigen IA-2 in INS-1 pancreatic beta-cells. Diabetes 49:1137–1141
20. Roberts C, Roberts GA, Löbner K, Bearzatto M, Clark A, Bonifacio E, Christie MR (2001) Expression of the protein tyrosine phosphatase-like protein IA-2 during pancreatic islet development. J Histochem Cytochem 49:767–776
21. Shimizu S, Saito N, Kubosaki A, SungWook S, Takeyama N, Sakamoto T, Matsumoto Y, Saeki K, Matsumoto Y, Onodera T (2001) Developmental expression and localization of IA-2 mRNA in mouse neuroendocrine tissues. Biochem Biophys Res Commun 288:165–171
22. Steinbrenner H, Nguyen T, Wohlrab U, Scherbaum WA, Seissler J (2002) Effect of proinflammatory cytokines on gene expression of the diabetes-associated autoantigen IA-2 in INS-1 cells. Endocrinology 143:3839–3845
23. Löbner K, Steinbrenner H, Roberts GA, Ling Z, Huang G, Piquer S, Pipeleers DG, Seissler J, Christie MR (2002) Different regulated expression of the tyrosine phosphatase-like proteins IA-2 and phogrin by glucose and insulin in pancreatic islets: relationship to development of insulin secretory responses in early life. Diabetes 51:2982–2988
24. Gross S, Blanchetot C, Schepens J, Albet S, Lammers R, den Hertog J, Hendriks W (2002) Multimerization of the protein-tyrosine phosphatase (PTP)-like insulin-dependent diabetes mellitus autoantigens IA-2 and IA-2beta with receptor PTPs (RPTPs). Inhibition of RPTPalpha enzymatic activity. J Biol Chem 277:48139–48145
25. Chin C, Sachs JN, Engelman DM (2005) Transmembrane homodimerization of receptor-like protein tyrosine phosphatases. FEBS Lett 579:3855–3858
26. Primo ME, Klinke S, Sica MP, Goldbaum FA, Jakoncic J, Poskus E, Ermácora MR (2008) Structure of the mature ectodomain of the human receptor-type protein-tyrosine phosphatase IA-2. J Biol Chem 283:4674–4681
27. Primo ME, Jakoncic J, Noguera ME, Risso VA, Sosa L, Sica MP, Solimena M, Poskus E, Ermácora MR (2011) Protein-protein interactions in crystals of the human receptor-type protein tyrosine phosphatase ICA512 ectodomain. PLoS ONE 6:e24191
28. Bork P, Patthy L (1995) The SEA module: A new extracellular domain associated with O-glycosilation. Protein Sci 4:1421–1425
29. Primo ME, Sica MP, Risso VA, Poskus E, Ermácora MR (2006) Expression and physicochemical characterization of an extracellular segment of the receptor protein tyrosine phosphatase IA-2. Biochim Biophys Acta 1764:174–181
30. Noguera ME, Primo ME, Sosa LNF, Risso VA, Poskus E, Ermácora MR (2013) Biophysical characterization of the membrane-proximal ectodomain of the receptor-type protein-tyrosine phosphatase phogrin. Protein Pept Lett 20:1009–1017
31. Humprey W, Dalke A, Schulten K (1996) VMD: visual molecular dynamics. J Mol Graph 14:33–38
32. Dundas J, Ouyang Z, Tseng J, Binkowski A, Turpaz Y, Liang J (2006) CASTp: computed atlas of surface topography of proteins with structural and topographical mapping of functionally annotated residues. Nucleic Acids Res 34:W116–W118
33. Dolinsky TJ, Nielsen JE, McCammon JA, Baker NA (2004) PDB2PQR: an automated pipeline for the setup of Poisson-Boltzmann electrostatics calculations. Nucleic Acids Res 32:W665–W667
34. Li H, Robertson AD, Jensen JH (2005) Very fast empirical prediction and rationalization of protein pKa values. Proteins 61:704–721
35. Otwinowski Z, Minor W (1997) Processing of X-ray diffraction data collected in oscillation mode. Methods Enzymol 276:307–326
36. Vagin A, Teplyakov A (2010) Molecular replacement with MOLREP. Acta Crystallogr D Biol Crystallogr 66:22–25
37. Keegan RM, Winn MD (2007) MrBUMP: an automated pipeline for molecular replacement. Acta Crystallogr D Biol Crystallogr 64:119–124
38. Winn MD, Ballard CC, Cowtan KD, Dodson EJ, Emsley P, Evans PR, Keegan RM, Krissinel EB, Leslie AGW, McCoy A, McNicholas SJ, Murshudov GN, Pannu NS, Potterton EA, Powell HR, Read RJ, Vagin A, Wilson KS (2011) Overview of the CCP4 suite and current developments. Acta Crystallogr D Biol Crystallogr D67:235–242
39. Murshudov GN, Skubák P, Lebedev AA, Pannu NS, Steiner RA, Nicholls RA, Winn MD, Long F, Vagin AA (2011) REFMAC5 for the refinement of macromolecular crystal structures. Acta Crystallogr D Biol Crystallogr 67:355–367
40. Emsley P, Cowtan K (2004) Coot: model-building tools for molecular graphics. Acta crystallographica. Acta Crystallogr D Biol Crystallogr 60:2126–2132
41. Painter J, Merritt EA (2006) TLSMD web server for the generation of multi-group TLS models. J Appl Crystallogr 39:109–111
42. Chen VB, Arendall WB, Headd JJ, Keedy DA, Immormino RM, Kapral GJ, Murray LW, Richardson JS, Richardson DC (2009) MolProbity: all-atom structure validation for macromolecular crystallography. Acta Crystallogr D Biol Crystallogr 66:12–21
43. Andreeva A, Howorth D, Chothia C, Kulesha E, Murzin A (2014) SCOP2 prototype: a new approach to protein structure mining. Nucleic Acids Res 42:D310–D314
44. Macao B, Johansson DG, Hansson GC, Hard T (2005) Autoproteolysis coupled to protein folding in the SEA domain of the membrane-bound MUC1 mucin. Nat Struct Mol Biol 13:71–76
45. Finn RD, Bateman A, Clements J, Coggill P, Eberhardt RY, Eddy SR, Heger A, Hetherington K, Holm L, Mistry J, Sonnhammer ELL, Tate J, Punta M (2014) Pfam: the protein families database. Nucleic Acids Res 42:D222–D230
46. Maeda T, Inoue M, Koshiba S, Yabuki T, Aoki M, Nunokawa E, Seki E, Matsuda T, Motoda Y, Kobayashi A et al (2004) Solution structure of the SEA domain from the murine homologue of ovarian cancer antigen CA125 (MUC16). J Biol Chem 279:13174–13182
47. Bozic D, Sciandra F, Lamba D, Brancaccio A (2004) The structure of the N-terminal region of murine skeletal muscle α-dystroglycan discloses a modular architecture. J Biol Chem 279:44812–44816
48. Duddy WJ, Nissink JWM, Allen FH, Milner-White EJ (2004) Mimicry by asx-and ST-turns of the four main types of β-turn in proteins. Protein Sci 13:3051–3055